Biophysical Chemistry 8 (1978) 1–15

LINEAR DICHROISM STUDIES OF BINDING SITE STRUCTURES IN SOLUTION. COMPLEXES BETWEEN DNA AND BASIC ARYLMETHANE DYES

Bengt NORDÉN, Folke TJERNELD and Eric PALM
Divisions of Biochemistry and Inorganic Chemistry, University of Lund, Chemical Center, S-220 07 Lund, Sweden

Received 26 September 1977
Revised manuscript received 10 November 1977

The interaction between B-form DNA and twelve cationic triaryl-methane dyes was studied with respect to optical properties and stabilities, using linear dichroism (LD) and aqueous two-phase partition techniques. Monovalent dyes derived from crystal violet as a rule form a single strong complex (K_1 ca $10^5\ M^{-1}$; site density per nucleotide base n_1 ca 0.1 at 0.1M ionic strength) in which the plane of the dye is at an angle of less than 50° to the local DNA helix axis. The complex with fuchsin is weaker ($10^4\ M^{-1}$) but can be explained by a similar orientation. For some of the dyes (those with pseudo-C_{2v} symmetry) the angular orientations of two molecule-fixed axes can be obtained. For the divalent methyl green a second complex appears to be formed at low ionic strength. Methyl green (and to some extent 2-thiophene green and malachite green) show exciton splitting in the LD spectrum and circular dichroism assignable to exciton coupling between transition dipoles roughly parallel to the helical strands, indicating a dye–dye interaction. The optical data, supported by fitting experiments with space-filling models, suggests a general structure for the binding site. The dye is not intercalated but is bound to exposed hydrophobic regions in the major groove. The ligand is in part (the charged amino groups) in contact with the phosphoribose chain but its main surface lies against the hydrophobic base-pair stack. For a *di*phenylmethane dye, Michler's hydrol blue, a perpendicular orientation was observed, possibly due to intercalation.

1. Introduction

The interaction between tripnenylmethane dyes and DNA has drawn considerable interest. Methyl green (MG) has long been used to monitor DNase activity and has recently been found to inhibit DNA synthesis [1]. Krey and Hahn [2] have used methyl green in studies of the binding of other agents to DNA. Gautier and Müller [3] have studied base-pair preferences of some triphenyl-methane dyes.

There has been some debate [2–4] about whether methyl green binds by intercalation but the structures of these complexes in solution have hitherto been little known.

While considerable information on biopolymers has been obtained from X-ray crystal studies there is relatively little information available from solution studies. Optical properties, particularly circular dichroism, have been used to monitor conformational changes in solution, but they usually do not yield more detailed structural information. However, important structural conclusions can often be drawn from measurements of linear dichroism (LD) of partially oriented solutions (using DNA solutions subjected to flow or electric fields [5,6]; in stretched films of solid DNA [7]; see also [8–13]). As yet only a limited number of workers have used LD for these purposes. In a recent communication [14] we showed that dyes, for instance methyl green, in which transitions of orthogonal polarizations have been established, provide more detailed information about the structure of complexes with biopolymers. In the present work we have utilized the "two-dimensional chromophore" nature of methyl green, and a number of related dyes, for investigation of the structure of the binding sites. The following dyes were studied: methyl green (MG^{2+}), malachite green (MAG^+), 2-thiophene green ($2\text{-}TG^+$). 3-pyridine green ($3\text{-}PC^+$), p-hydroxymalachite green ($p\text{-}OH\text{-}MAG^+$), p-nitromalachite green ($p\text{-}NO_2MAG^+$), o-methoxymalachite green ($o\text{-}CH_3O\text{-}MAG^+$), p-methoxymalachite green ($p\text{-}CH_3O\text{-}MAG^+$), o-bromomalachite green ($o\text{-}Br\text{-}MAG^+$), p-iodomalachite green ($p\text{-}I\text{-}MAG^+$), crystal violet (CV^+), p-fuchsin ($p\text{-}F^+$) and Michler's hydrol blue ($MICH^+$).

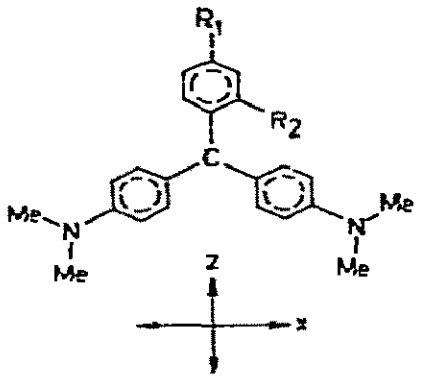

MAG$^+$ $R_1 = R_2 = H$
p-OH-MAG$^+$etc R_1 = OH etc
o-OCH_3-MAG$^+$etc $R_2 = OCH_3$ etc

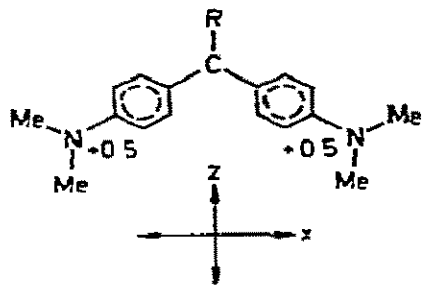

MICH$^+$: R=H
3-TG$^+$ R= 2-thienyl
3-PG$^+$ R= 3-pyridyl

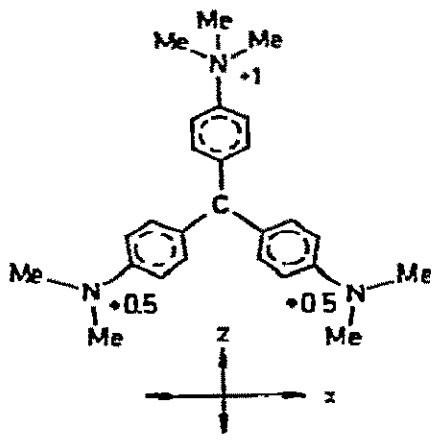

MG^{2+}

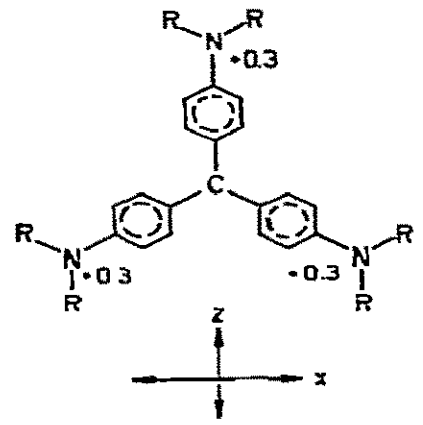

CV$^+$: R=Me
F$^+$: R=H

In previous work [12] we relied upon a theoretical orientation to the Peterlin-Stuart distribution, which presumes rigid particles. Here, we have used an approach that is formally different for estimating the orientation (vide infra).

2. The theoretical basis for dynamic dichroism

The linear dichroism of a rigid particle in a hydrodynamic gradient is relatively easy to interpret provided the orientational distribution function for the system is known. For example, if the molecules can be represented as ellipsoids of revolution, the Peterlin-Stuart distribution [15] may be employed, leading to a well established relationship between the observed linear dichroism of the flowing solution with the dichroism tensor of the molecules themselves [6,16]. The linear dichroism

$$\mathrm{LD} = A_Z - A_X = C \cdot d \cdot (\epsilon_Z - \epsilon_X) \qquad (1)$$

of a solution of an orientable species of concentration C, with an optical pathlength d, is then given simply by

$$\frac{\mathrm{LD}}{A_r} = \frac{\epsilon_Z - \epsilon_X}{\epsilon_r} = F(G/D, p) \cdot \tfrac{3}{2} \,(3\,\langle\cos^2\theta\rangle - 1). \qquad (2)$$

Dividing by the absorption of the solution at rest, enables C and d and other constants relating the absorption to dipole strength to be eliminated. F is an orientational factor, $0 \leqslant F \leqslant 1$, given by the Peterlin-Stuart distribution for a given mode of optical propagation (in the present study we have employed a radial observation through the Couette cell). Its value can be obtained from the tables of Scheraga et al. [17] and Wada [6] as a function of the reduced gradient G/D (G = flow gradient across the cylindrical gap in the flow cell, D = rotary diffusion constant of the molecule), and the axial ratio $p = a/b$ (a and b are the lengths of the major and the minor axes of the ellipsoid). θ denotes the angle that the transition moment makes with the molecular orientation axis (= major axis). We here assume that there is only a single transition absorbing at the wavelengths of interest (in the case where there are overlapping bands with differing polarizations the second, "optical factor", of eq. (2) becomes instead a sum over the various transitions).

Eq. (2) has been applied in studies of DNA [6,12] but is strictly not valid for this and other flexible biopolymers, whose orientational and optical properties have to be derived as averages over the internal conformational angles rather than from a rigid molecular framework. To obtain the dichroism, we must have information on the orientational factor, preferably according to the theory of Zimm-Rouse for flexible chains, and also on the mode of molecular extension, at a given shear gradient. The rapidly increasing theoretical complexity in such cases has, however, deterred many workers from using this model and has made them overlook the errors involved in the application of the rigid ellipsoid model.

Wilson and Schellman have recently derived a statistical theory for the dichroic tensor of flexible helices [18]. They show that for a DNA-like (= fairly stiff) chain the molecular dichroism is given as a product of the dichroism of a segment, $\Delta\epsilon_l$, and the factor $(P_\infty/l)(r^2/\langle r^2\rangle_0$, where r is the length of the end-to-end vector of the chain, P_∞ the persistence length (for B-form DNA around 500 Å) and l the length of each segment (3.4 Å). At $G = 0$ when r^2 becomes equal to

$\langle r^2\rangle_0$, the chain dichroism is $(P_\infty/l)\,\Delta\epsilon_l$. The chain has statistically axial symmetry around its orientation direction, z, and for a hypothetical ensemble of completely oriented chains the polarized absorption may be written as

$$\epsilon_i = \boldsymbol{E}_i^{\mathrm{T}}\,\boldsymbol{O}^{\mathrm{T}} \begin{pmatrix} \epsilon_{\perp z} & 0 & 0 \\ 0 & \epsilon_{\perp z} & 0 \\ 0 & 0 & \epsilon_{\parallel z} \end{pmatrix} \boldsymbol{O}\boldsymbol{E}_i . \qquad (3)$$

where $\boldsymbol{E}_i$ is a unit vector in the laboratory system (X, Y, Z) denoting the direction of polarization. $\boldsymbol{O}$ is a transformation matrix, composed of the direction cosines of the laboratory axes and those of a given molecule. T means the transpose. Taking $\Delta\epsilon_{\mathrm{chain}} = \epsilon_{\parallel z} - \epsilon_{\perp z}$ and averaging with respect to the orientational distribution one obtains

$$\epsilon_Z - \epsilon_X = \Delta\epsilon_l \frac{P_\infty}{l} \frac{r^2}{\langle r^2\rangle_0} \{\langle\cos^2 Zz\rangle - \langle\cos^2 Xz\rangle\} \qquad (4)$$

where Zz and Xz denote the angles between the molecular z axis and the laboratory axes Z and X, respectively. Eq. (4) shows that the macroscopic dichroism is factored into optical and geometrical parts. In DNA we may assign a local helix axis, H, to the smallest part (at least one base-pair) in which the helix can be considered straight. If θ^{H} is the angle the transition moment makes with this axis we may write eq. (4) as follows:

$$\frac{\mathrm{LD}}{A_r} = \frac{\epsilon_Z - \epsilon_X}{\epsilon_r} = F^{\mathrm{do}}\,\tfrac{3}{2}\,(3\cos^2\theta^{\mathrm{H}} - 1)$$

$$0 \leqslant \theta^{\mathrm{H}} \leqslant 90^\circ, \qquad (5)$$

F^{do} is a weighting function taking into account the average molecular deformation and orientation, at a given gradient.

Due to the complicated nature of F^{do}, this parameter is conveniently determined empirically from the LD/A_r of a band for which θ^{H} is known. In the present study of complexes with DNA, the intrinsic base absorption was used for this purpose. When F^{do} has been established for DNA for a given degree of complexation with a ligand L and for a fixed flow gradient, eq. (5) can then be applied to an absorption in L with known polarization to give the angular orientation (θ^{H}) of the corresponding direction in L with respect to the local helix axis. The LD/A_r to be inserted, should refer to pure complex and preferably to a defined site, S(i). If the equilibrium analysis permits detailed mapping of the various species S(i) L, it should be possible to characterize any site i by the way in which it orients L, using the ratio

$$\frac{\Delta\epsilon_i(\lambda)}{\epsilon_i} = \frac{\mathrm{LD} - d\,\Sigma_{j\neq i}[\mathrm{S}(j)\,\mathrm{L}]\,\Delta\epsilon_j(\lambda)}{A - d\,\Sigma_{j\neq i}[\mathrm{S}(j)\,\mathrm{L}]\,\epsilon_j(\lambda)}, \qquad (6)$$

where $\Delta\epsilon_i(\lambda)$ is the specific ($\mathrm{M^{-1}\,cm^{-1}}$) linear dichroism at the wavelength λ of L when bound at site i at some standard gradient, and $\epsilon_i(\lambda)$ is the corresponding ordinary absorption coefficient (random solution).

3. Equilibrium analysis

As a first approach it is reasonable to assume that complex formation between a site S(i) on DNA and a ligand, L,

$$\mathrm{S}(i) + \mathrm{L} \rightleftharpoons \mathrm{S}(i)\,\mathrm{L}, \qquad (7)$$

$$K_i = \frac{[\mathrm{S}(i)\,\mathrm{L}]}{[\mathrm{S}(i)]\,[\mathrm{L}]}, \qquad (8)$$

contributes to linear dichroism and absorbance in the absorption region of L according to:

$$\mathrm{LD}(\lambda) = \sum_i [\mathrm{S}(i)\,\mathrm{L}]\,d\Delta\epsilon_i(\lambda), \qquad (9)$$

$$A(\lambda) = \sum_i [\mathrm{S}(i)\,\mathrm{L}]\,d\epsilon_i(\lambda) + [\mathrm{L}]\,d\epsilon_{\mathrm{L}}(\lambda). \qquad (10)$$

The fact that $\Delta\epsilon_{\mathrm{L}}$ is 0 (since L is too small a molecule to be oriented by the gradient used) means that a finite LD is an unequivocal criterion for the existence of a complex. Experience shows that cubic chromophores, or ligands bound without any specific orientation, exhibit some LD when attached to a flow-oriented biopolymer [19]. Absence of LD may therefore in general be taken as firm evidence of the absence of binding. The method of detecting LD imposes however a limit (with our method 10^{-8} M S(i) L).

To be able to use the observed LD for quantitative interpretation it is desirable to determine the amounts of the pertinent species which are present in the particular solution. This equilibrium analysis can in principle be performed in two ways, regardless of the experimental properties employed; one of these is suit-

able for graphic evaluation. In the first, the observed property (here LD) is expressed in known and unknown parameters and the latter are computationally varied to minimize the difference between theoretical and experimental observable. In the second, one starts with an estimate of the ligand number

$$r \equiv (C_L - [L])/C_N, \tag{11}$$

where the total concentrations of ligand and nucleotides are

$$C_L = [L] + \sum_i [S(i)L], \tag{12}$$

$$C_N = C_{S(i)}/n_i = \sum_i ([S(i)] + [S(i)L])/n_i. \tag{13}$$

Obviously r can be expressed in terms of the desired K_i and n_i:

$$r = \sum_i \frac{n_i K_i [L]}{1 + K_i [L]}. \tag{14}$$

In the case of a single class of binding sites, a plot of $r/[L]$ versus r yields a straight line with the intercept at r equal to n_1 on the r axis and with the slope equal to $-K_1$.

$$r/[L] = n_1 K_1 - K_1 r. \tag{15}$$

Usually such plots (Scatchard plots) are not linear but are curved at higher r due to the formation of "higher complexes". These may correspond to other geometrical sites but may also be created by a decreased free energy gain at the original site due to the electrostatic interaction from neighbouring bound ligands (usually called negative cooperativity). In the case where two discrete binding classes can be distinguished, corresponding to the stabilities K_1 and K_2, and $K_1 \gg K_2$, it follows from eq. (14) that the $r/[L]$ versus r plot at low r should exhibit a linear portion which has the slope $-K_1$ and the intercept $r/[L] = K_1 n_1 + K_2 n_2$ at $r = 0$ but at high r should have a different linear portion with the slope $-K_2$ and the intercept $r = n_1 + n_2$ at $r/[L] = 0$.

Eq. (15) is useful in "free ligand" measurements (equilibrium dialysis, partition methods) but for estimating the stability from the LD in the case of a single class of binding sites, it is more convenient to use the method suggested in ref. [12]. When the sites S(1) are completely occupied LD reaches a saturation value, LD_{max}. A ligand number $\bar{n} = [SL]/C_S$ [12] is then obtained as LD/LD_{max} for any point on the titration curve. With only one stability constant, K_1, a plot of $1/(1-\bar{n})$ versus $C_L/\bar{n}$ yields a straight line with K_1 as the slope and $n_1 C_N$ as the intercept at $1/(1-\bar{n}) = 0$ (eq. (9) in ref. [12]).

4. Experimental

LD was measured as before on DNA solutions oriented in a Couette device [12,13]. Circular dichroism (measured in a Jasco J-41 spectrometer) is given in absorbance units, $CD = A_l - A_r = (\epsilon_l - \epsilon_r) Cd$ where $\epsilon_l - \epsilon_r$ is in $M^{-1} cm^{-1}$.

The partition method used in the equilibrium studies is that described by Albertsson [20,21]. A two-phase system of 4% polyethylene glycol ("PEG 6000") and 5% dextran ("dextran 500") in water was employed. We found that DNA is quantitatively taken up by the bottom (dextran) phase when 5 mM NaAc + x mM NaCl ($0 \leqslant x \leqslant 100$), is used as ionic medium. A constant pH = 5.0 was used to keep the dyes in the cationic forms indicated. The partition coefficients for the different ligands were determined spectrophotometrically as $K_p = C_L$ (top phase)$/C_L$ (bottom phase) in the absence of DNA at the appropriate ionic strengths. K_p varied between 1.19 and 1.48. For the DNA-L equilibrium experiments a set of test tubes was arranged with varying C_L and a constant DNA concentration. After shaking, the phases were allowed to separate (ca 1 h) and the free ligand concentration in the bottom phase was obtained from the absorbance of the top phase.

Calf thymus DNA (Sigma type I) was used; the concentration (C_N) was determined from the UV absorbance ($\epsilon_{260\,nm} = 6600\ M^{-1} cm^{-1}$). The triphenylmethane dyes were kindly donated to us by Cigén and Bengtsson (syntheses and analyses according to [22] and references therein). The concentrations of the dyes were determined spectrophotometrically.

5. Results and discussion

An understanding of the optical properties of complexes between a ligand and a macromolecule requires characterization of the optical properties of the separate species. The dyes used may be divided into two

classes: those which can be considered as having C_{2v} symmetry (MAG and its derivatives, MG etc) and those which have essentially C_{3v} symmetry (CV, F). (Since the molecules, for steric reasons, are non-planar, the symmetries are probably more precisely C_2 and D_3, respectively.) From group theory it follows that any transition in these molecules must be polarized along either the z or the x axis (C_{2v}, C_2) or have degenerate xz polarization (C_{3v}, D_3). Any significant out-of-plane polarization can be ignored. Methyl green can be taken as a representative of the first class. Like all the others in this group, methyl green displays a characteristic pair of bands: one band centred at 430 nm which is unequivocally known to have z polarization [23] and one band around 640 nm, which is more or less purely x polarized. In a recent study of dyes oriented in polyvinyl alcohol [23], the component spectra of the absorption tensor were resolved using the assumption of negligible out-of-plane intensity. According to this resolution, the 640 nm bands in MAG and MG should have a considerable admixture of z polarized intensity.

Complexation between the dyes and flow-oriented DNA manifests itself by a more or less intense LD signal corresponding to the energy of the dye absorption. Since most of the dyes give complexes with stabilities of at least $10^5\ M^{-1}$, it is easy to find a C_N and a C_L where practically the entire amount of added dye is bound, and there is a low degree of occupation of the available sites. $\Delta\epsilon_1/\Delta\epsilon_1$ can then be obtained as a very good approximation as the ratio between the directly recorded LD and A. Further, since DNA is in great excess and since most of the dyes have no absorption at the wavelength of the intrinsic DNA absorption, it follows that $(LD/A)_{257\ nm}$ gives the value of F^{do} via eq. (5) directly, by inserting $\theta^H = 90°$. Table 1 summarises the LD results.

Let us consider the MG-DNA complex and the associated optical properties (fig. 1). Irrespective of whether the band at 640 nm (645 nm in DNA complex, 632 in aqueous solution) is purely x polarized or not, the fact that it shows positive LD in the flow-oriented complex excludes the possibility of intercalation involving the x direction. On the other hand, the large LD/A at 425 nm (the amplitude is actually even larger than that of the intrinsic base absorption at 257 nm) demonstrates that the z direction in MG is practically perpendicular to the local helix axis. This orientation

Table 1
Observed LD and LD/A of the dye-DNA complexes at the characteristic LD extrema. $I = 0.10$ M NaCl, $C_N = 4.0 \times 10^{-4}$ M DNA phosphate, $G = 4000\ s^{-1}$. C_L/C_N given in the first column

L (C_L/C_N)	Wavelength of LD extremum (nm)	$LD \times 10^3$ ($d = 0.10$ cm)	LD/A [a]
MG^{2+}	257	−40.00	−0.154
(0.025)	310	−7.0	−0.17
	425	−2.67	−0.181
	645	5.09	+0.062
MAG^+	257	−36.70	−0.115
(0.043)	430	−3.52	−0.100
	630	5.94	+0.036
2-TG^+	257	−38.18	−0.103
(0.043)	470	−4.30	−0.075
	640	3.27	0.023
3-PG^+	257	−45.15	−0.173
(0.026)	425	−1.97	−0.119
	645	3.39	0.043
p-OH-MAG^+	257	−40.91	−0.156
(0.026)	455	−2.58	−0.112
	625	2.82	0.042
p-NO_2-MAG^+	257	−40.90	−0.154
(0.026)	425	−1.82	−0.106
	650	2.82	0.045
o-CH_3O-MAG^+	257	−33.94	−0.133
(0.025)	430	−0.33	−0.023
	640	0.88	0.013
p-CH_3O-MAG^+	257	−36.36	−0.141
(0.025)	455	−2.73	−0.110
	625	2.27	0.031
o-Br-MAG^+	257	−33.03	−0.129
(0.025)	420	−1.24	−0.083
	645	3.24	0.037
p-I-MAG^+	257	−37.88	−0.146
(0.025)	435	−2.11	−0.102
	635	2.23	0.030
CV^+	257	−35 5	−0.120
(0.040)	550	−3.62	(−0.032) [b]
	593	−2.74	(−0.018) [b]
	(640)	+	+
p-F^+	257	−33.6	−0.130
(0.025	315	+0.76	(+0.048) [b],[c]
	500	−0.84	(−0.010) [b],[c]
	545	−0.70	(−0.005) [b],[c]
	635	- 0.04	(+0.02) [b],[c]

[a] Generally $LD/A \approx (\Delta\epsilon/\epsilon)_{S(1)L}$; Exceptions: crystal violet and p-fuchsin.
[b] Not equal to $\Delta\epsilon/\epsilon$ due to incomplete complex formation.
[c] It was possible to run F^+-DNA in dextran (the bottom phase from a partition experiment, diluted with 3% H_2O) at I = 0.01 M Na^+, $C_L/C_N = 0.12$, $C_N = 3.6 \times 10^{-4}$ M $(LD/A)_{257} = -0.38$, $(LD/A)_{555} = -0.050$; corrected $(\Delta\epsilon/\epsilon)_{555} = -0.19$.

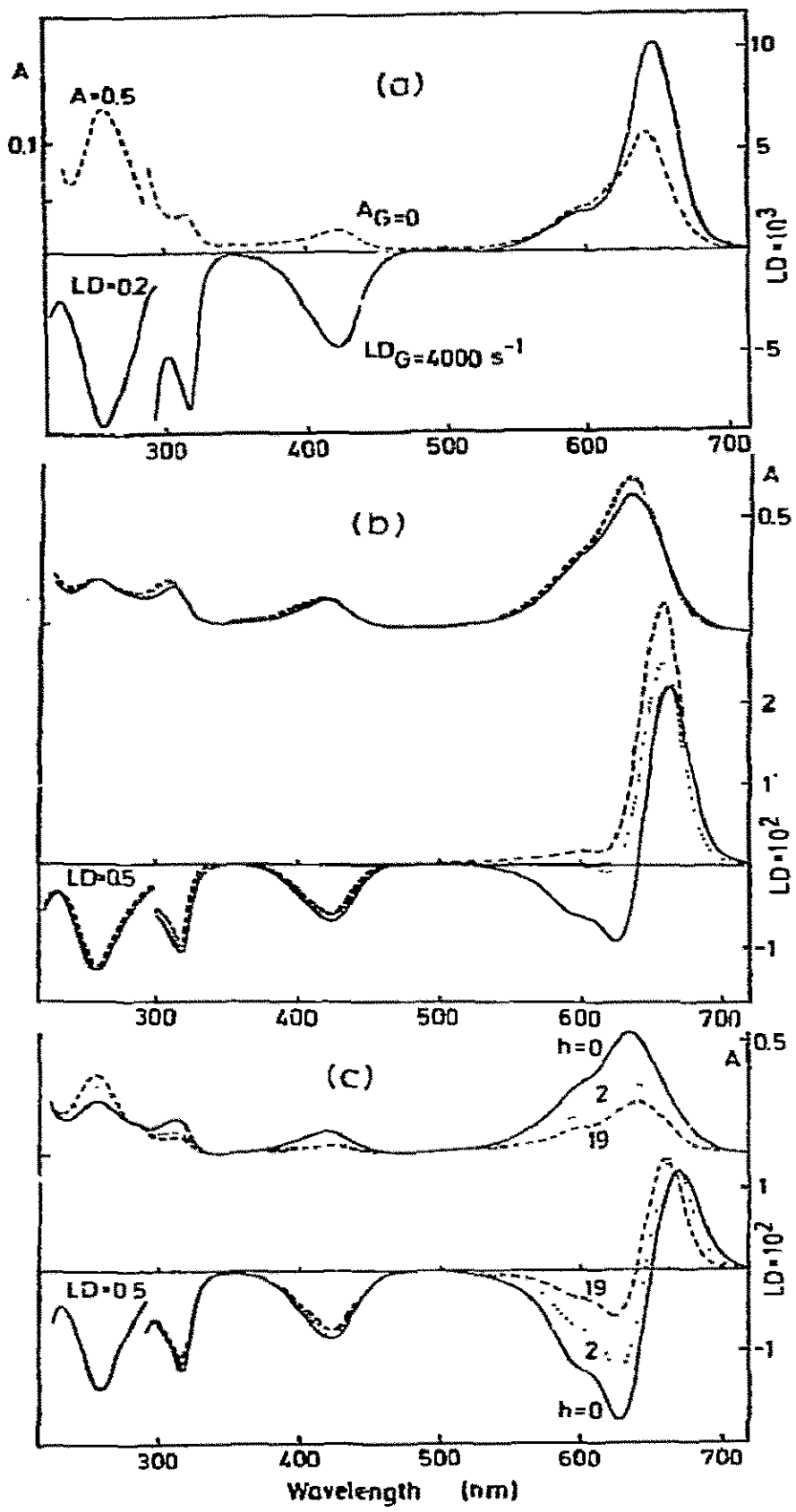

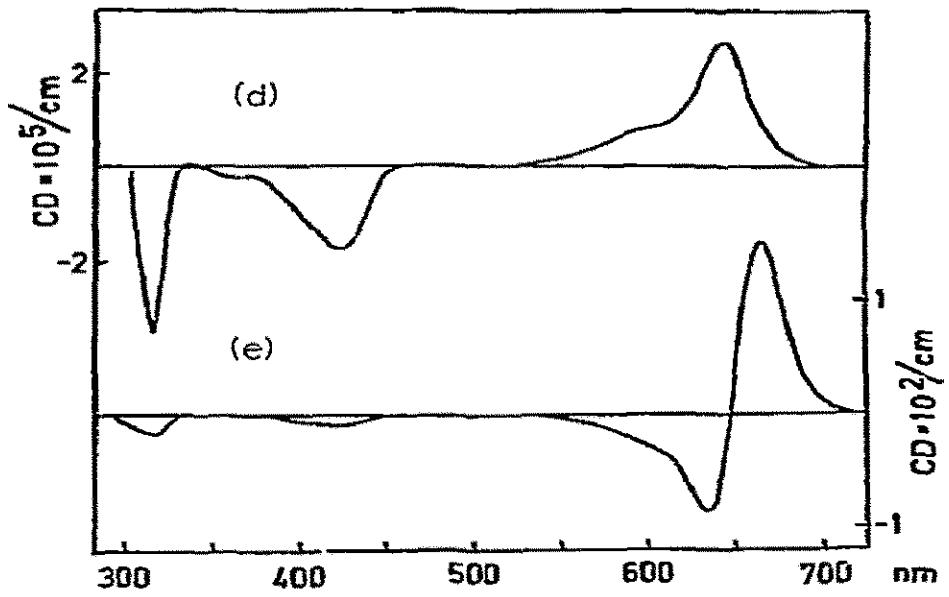

Fig. 1. (a)–(c) Linear dichroism (LD) and absorption (A) (G = 4000 s^{-1}, d = 0.10 cm) of DNA + MG. (a) at C_L/C_N = 0.026, $C_N = 3.9 \times 10^{-4}$ M, acetate buffer (5×10^{-3} M) pH = 5.0. (b) at C_L/C_N = 0.80 ($C_N = 2 \times 10^{-4}$ M), ionic strength $I = 5 \times 10^{-3}$ M (——, acetate buffer) and $I = 55 \times 10^{-3}$ M (···, addition of NaCl) and I = 0.1 M (– – –, addition of NaCl), (c) C_L/C_N = 0.80 ($C_N = 2 \times 10^{-4}$ M) and pH = 8.0 (curves at different times (h hours) after the addition of MG, 5 mM Tris-HCl buffer).
Fig. 1. (d)–(e) Circular dichroism of DNA + MG at $I = 5 \times 10^{-3}$ M (acetate buffer) and $C_N = 4.0 \times 10^{-4}$ M. (d) C_L/C_N = 0.0023, (e) C_L/C_N = 0.23.

could result if the trimethylaminophenyl group was intercalated. We shall return to this later.

As seen in fig. 1b, the LD spectrum of MG +DNA changes in a characteristic way when the ligand concentration is increased; a new band with negative sign arises at ca 630 nm. If a "complex" S(i) L is defined by its specific $\Delta\epsilon_i$, this band is evidence for the formation of at least one additional complex. The fact that the new band can be completely suppressed by increasing the ionic strength suggests that the higher complexes are of electrostatic nature. If the pH is raised from 5 to 8 in a solution of MG + DNA, MG is slowly converted to the corresponding carbinol, which is uncoloured. The concept of two complexes, is here supported by the observation (fig. 1c) that only the free ligand and the portion responsible for the negative LD at 630 nm, undergoes this change. In other words, MG bound in the first site retains its dye structure.

The positive long-wavelength band and the negative band at shorter wavelength are common for all the dyes with pseudo-C_{2v} symmetry (see table 1), with one exception: the dye Michler's hydrol blue, which is known to have pure x polarization at 605 nm and almost pure z polarization at 400 nm [23], showed an overall negative LD in its complex with DNA. Because of the uncertain stability, we have not reported the observed LD/A data.

The two pseudo-C_{3v} symmetry dyes, crystal violet and p-fuchsin, display a binding that is apparently more sensitive to the ionic strength than the other dyes. At I = 0.005 M Na^+ both precipitated the DNA.

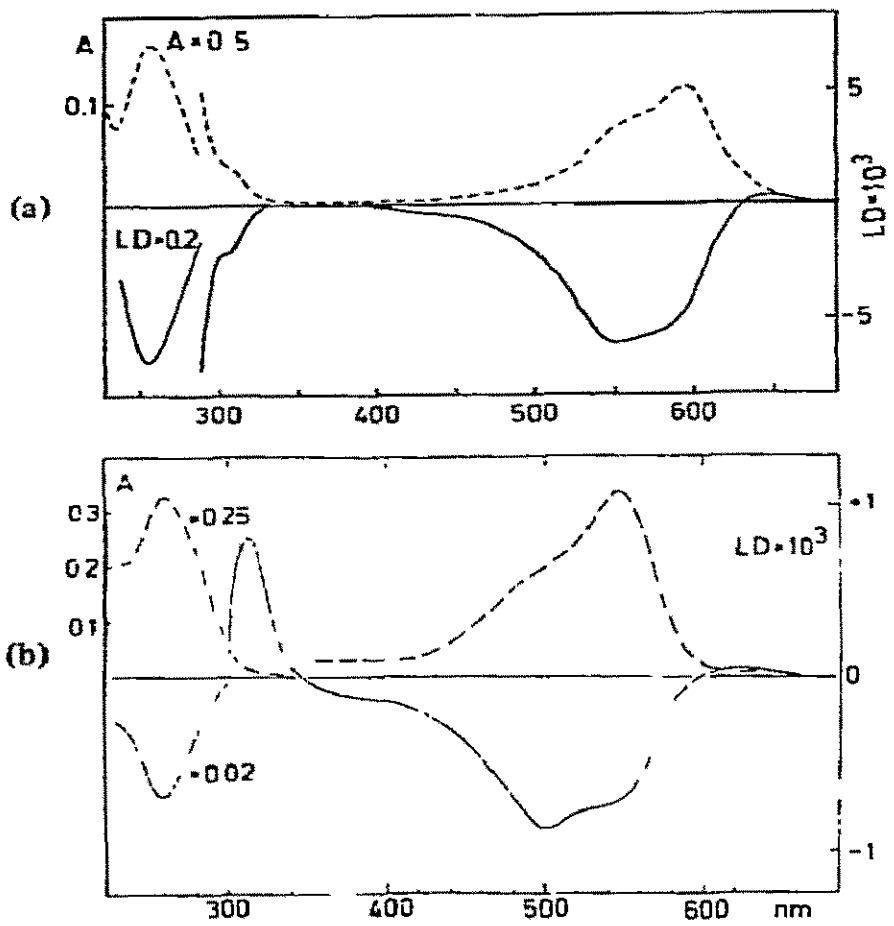

Fig. 2. LD (——, $G = 4000\ s^{-1}$, $d = 0.10$ cm) and A (– – –, $d = 1.0$ cm) of (a) crystal violet + DNA ($C_L = 1.0 \times 10^{-5}$ M, $C_N = 3.8 \times 10^{-4}$ M DNA phosphate, $I = 0.10$ M Na^+) (b) p-fuchsin + DNA ($C_L = 1.0 \times 10^{-5}$ M, $C_N = 4.0 \times 10^{-4}$ M, $I = 0.10$ M Na^+).

At $I = 0.1$ M Na^+ a certain precipitation occurred which prevented equilibrium measurements by partition, but a weak LD could be observed (fig. 2). With fuchsin, a study in dextran solution at $I = 0.01$ M (see note to table 1) showed that the $\Delta\epsilon/\epsilon$, corrected for non-bonded dye, amounted to a fairly large negative value. A positive LD band at 310 nm can be due to a partly out-of-plane polarized "^1L_b" residue of the twisted benzene rings. The polarization observed at this position in polyvinyl alcohol [23] is consistent with this.

Returning to MG and the equilibrium studies, the interpretation of the LD in terms of stabilities must clearly be very uncertain for an increasing degree of ligand occupation of the helix. Fig. 3 shows the LD titration curves at different C_N values and ionic strengths. With a high ionic strength (fig. 3c) the LD signals are in accord with the formation of a single complex only, and a $1/(1-\bar{n})$ plot yields a stability constant K_1 and a density number n_1 which agree reasonably well with those obtained from two-phase partition equilibrium analyses (table 2, $I = 0.1$ M). However, at low ionic strength (fig. 3a, b) all LD curves, except for that of the 425 nm band, show a non-monotonous behaviour due to the build-up of a second

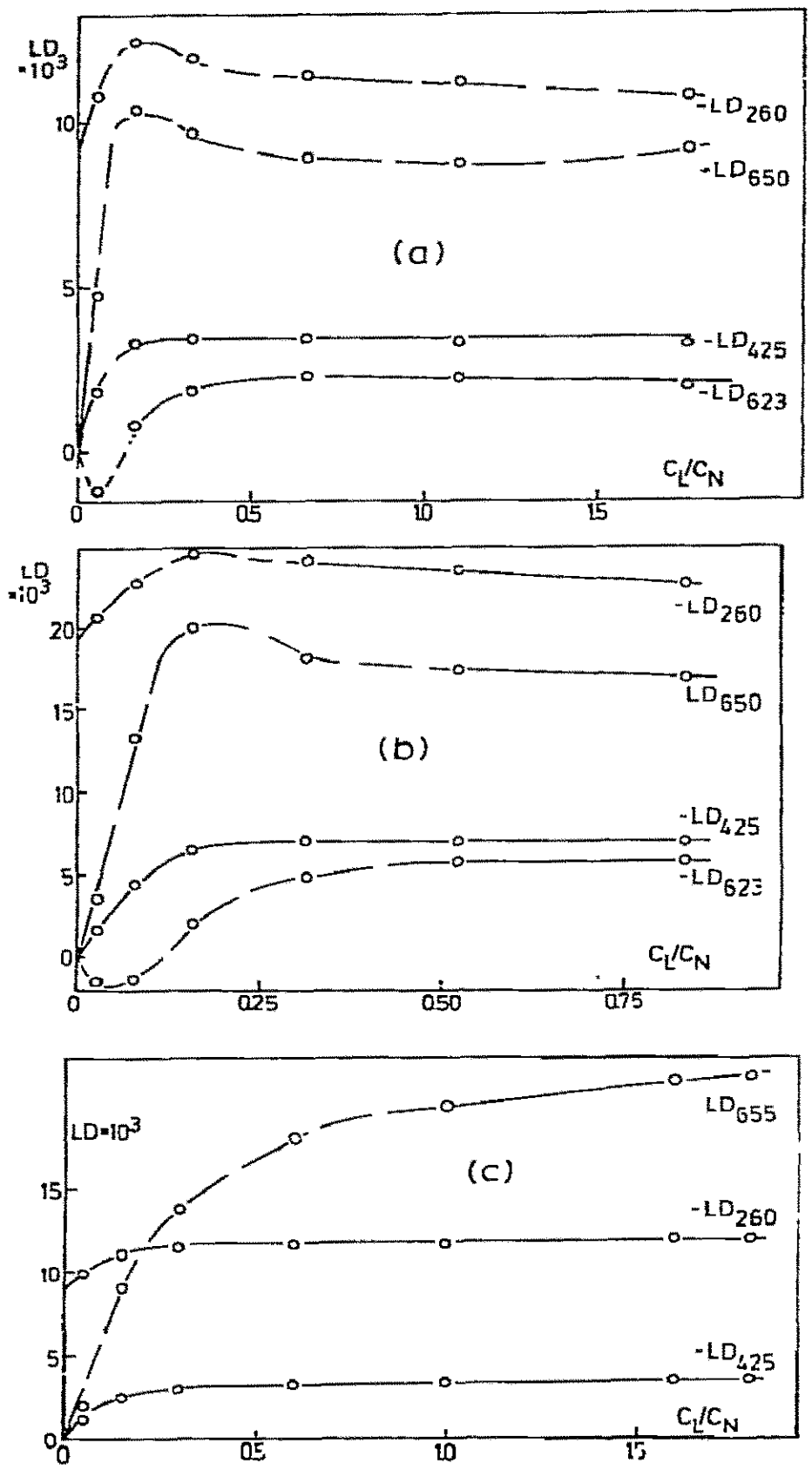

Fig. 3. Titration curves showing LD at the extrema as a function of C_L/C_N. L = MG^{2+}. (a) $I = 5.0 \times 10^{-3}$ M Na^+ (acetate buffer, pH = 5) $C_N = 0.92 \times 10^{-4}$ M (DNA phosphate). (b) $I = 5.0 \times 10^{-3}$ M Na^+, $C_N = 1.9 \times 10^{-4}$ M. (c) $I = 0.1$ M Na^+ (buffer + NaCl), $C_N = 1.0 \times 10^{-4}$ M.

Table 2
Stability data estimated from LD or from aqueous two-phase partition. The stability constants K_1, K_2 in 10^5 M^{-1}.

	From LD [a]		From partition	
L	I = 0.005 M	I = 0.10 M	I = 0.005 M	I = 0.10 M
MG^{2+}				
K_1	5.3 ± 4	2.0 ± 1	18 ± 3	3.2 ± 2
n_1	0.10 ± 0.05	0.08 ± 0.05	0.15 ± 0.02	0.10
K_2	(0.9)		(1)	(0.3)
n_2	(0.13)		(0.10)	(0.3)
MAG^+				
K_1	2.4			
n_1	0.04			
2-TG^+				
K_1	1.4	0.50	1.4	
n_1	0.04	0.06	0.02	
K_2			(0.2)	
n_2			(0.06)	
3-PG^+				
K_1	3.8	1.7		
n_1	0.09	0.15		
p-OH-MAG^+				
K_1	precipita-	1.0	precipita-	
n_1	tion	0.10	tion	
p-NO_2-MAG^+				
K_1	2.6			
n_1	0.09			
o-CH_3O-MAG^+				
K_1				0.80 ± 0.4
n_1				0.02 ± 0.01
p-CH_3O-MAG^+				
K_1				0.90 ± 0.4
n_1				0.06 ± 0.03
o-Br-MAG^+				
K_1		1.7		
n_1		0.12		
p-I-MAG^+				
K_1		8.3		
n_1		0.15		
CV^+	precipita-			
K_1	tion	(4.3) [b]		
n_1		(0.10) [b]		
p-F^+	precipita-			
K_1	tion	(0.01) [b,c]	0.2 [c] (I = 0.01 M)	

[a] Neglect of exciton coupling.
[b] The value is uncertain due to precipitation.
[c] Calculated on the assumption of n_1 = 0.10.

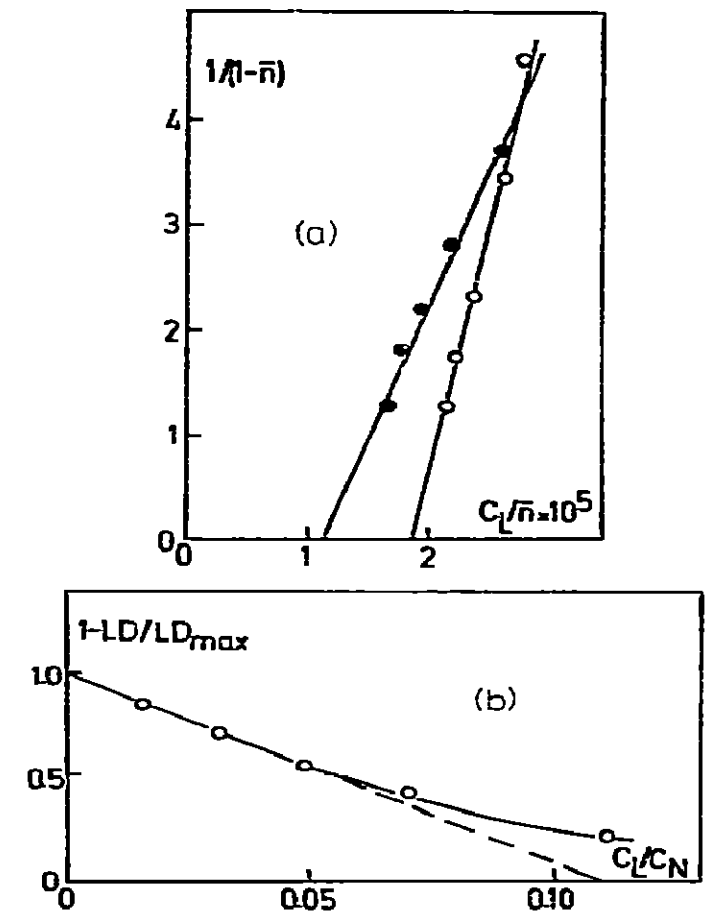

Fig. 4. (a) Evaluation of K_1 and n_1 for MG-DNA from the LD signal at 425 nm at low C_L (corresponding to fig. 3b, ○, and c, ●, and by means of eqs. (8) – (9) in ref. [12]). (b) Estimate of n_1 = lim (C_L/C_N) when $1 - LD/LD_{max} \rightarrow 0$.

complex at higher C_L/C_N. Fig. 4a,b, shows examples of graphical evaluations of K_1 and n_1.

The similarity between the LD versus C_L/C_N curves for different C_N, with extrema in the region C_L/C_N = 0.05, can be explained by two strong complexes. However, there are several indications that the changed character of the LD spectrum is due to an effect of interactions between dye molecules and does not necessarily require a different site for the second complex: 1. A characteristic exciton couplet is observed in circular dichroism at the position of the x polarized absorption in MG (fig. 1e) with a strong rotational strength compared to that of the "monomer" complex. No large circular dichroism is observed at the position of the z polarized band. This behaviour is consistent (see below) with a right handed helical array of MG: site 1 complexes. The circular dichroism intensity, as well as the LD adjusted for the estimated contribution from a "first complex" (fig. 5), show a quadratic behaviour as functions of C_L/C_N, as expected for the

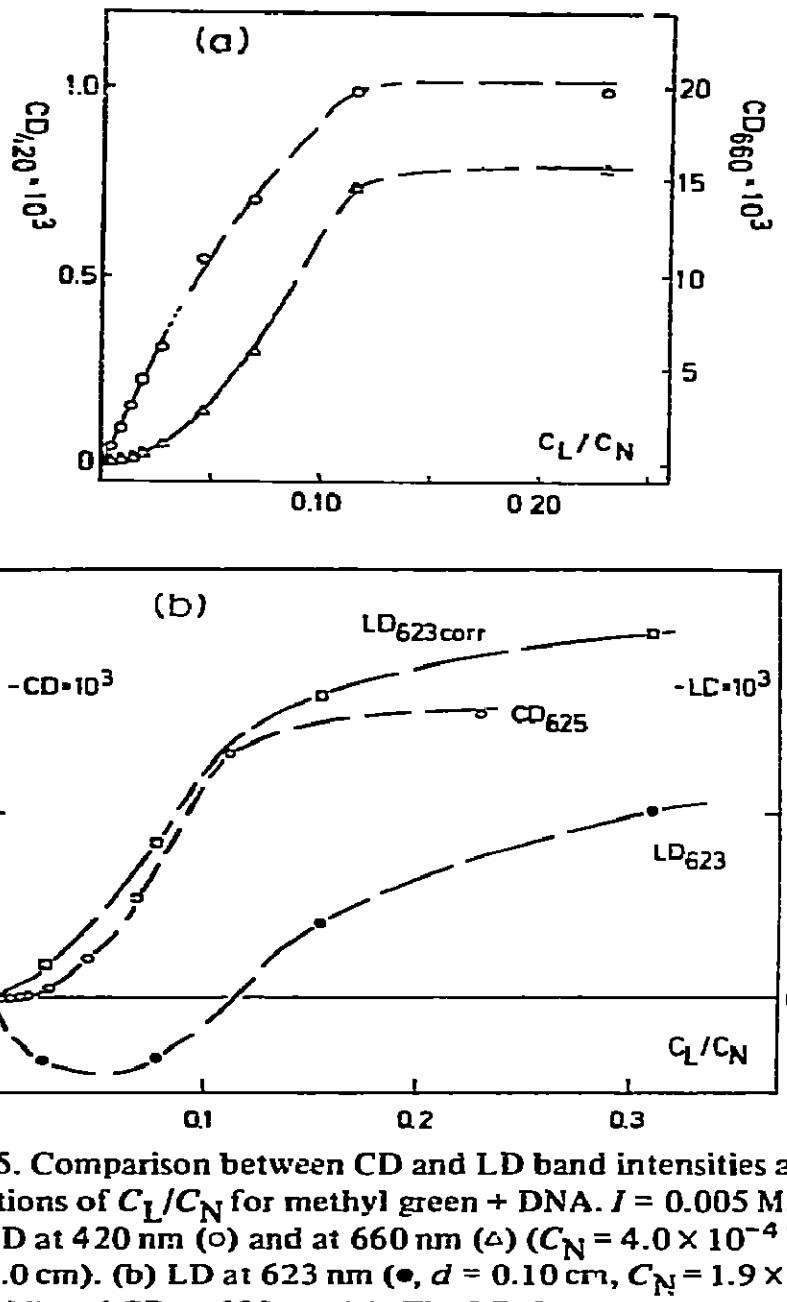

Fig. 5. Comparison between CD and LD band intensities as functions of C_L/C_N for methyl green + DNA. I = 0.005 M. (a) CD at 420 nm (○) and at 660 nm (△) ($C_N = 4.0 \times 10^{-4}$ M, d = 1.0 cm). (b) LD at 623 nm (●, d = 0.10 cm, $C_N = 1.9 \times 10^{-4}$ M) and CD at 625 nm (○). The LD due to exciton coupling is visualized (LD_{corr}, □) by subtracting the LD estimated for the non-interacting dye from LD_{623}.

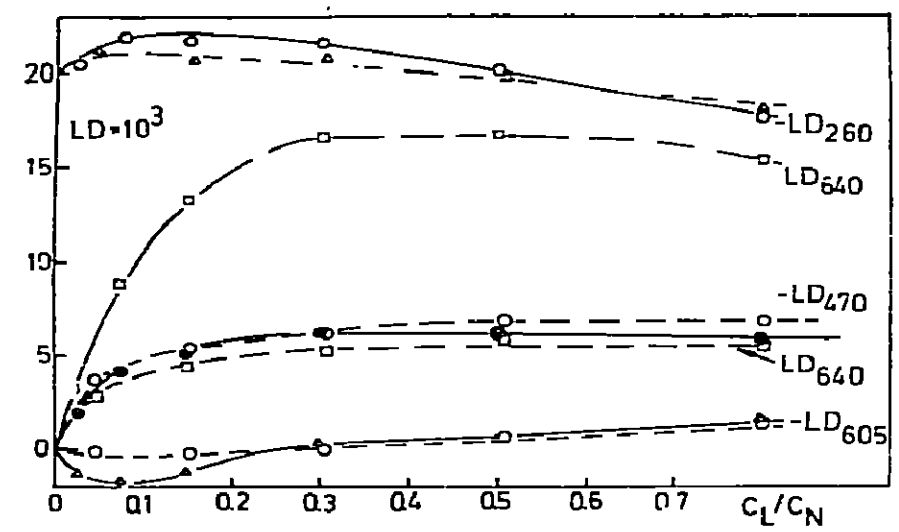

Fig. 6. Titration curves showing LD at the extrema as a function of C_L/C_N for 2-thiophene green (– – –) and for malachite green (——). $C_N = 2.0 \times 10^{-4}$ M, I = 0.005 M Na^+.

dipole–dipole intensity [24].

The concept of a single strong binding site gives a very simple account of these phenomena — it does not exclude "higher complexes", here collected in K_2, due to the successively changing electrostatic free energy. However, some details are difficult to understand:

1. The 425 nm LD peak (fig. 3a, b) reaches a saturation value while the other bands do not. This should indicate that later binding dye molecules have an almost zero $\Delta\epsilon/\epsilon$ at 425 nm, i.e. a more disordered arrangement of the z axis.

2. There appears not to be any correlation between the degree of dye–dye interaction (MG, MAG and possibly 2-TG are the only dyes with evidence for this, see figs. 6, 7) and the site density n_1. Such a correlation would be expected if the exciton effects were simply a result of a dense packing of dyes in the first site.

The intrinsic DNA LD at 257 nm can be used to follow the effect of complex formation on the DNA structure. Generally, an increase of 10–20% in LD/A at low C_L/C_N indicates a corresponding increase in F^{do} (since the optical factor in B-form DNA has a θ^H close to 90° the effect cannot originate from a changed base structure or from perturbed base polarizations). F^{do} is most probably increased by an increased persistence as the helix is filled with dye molecules. At higher ligand occupation a more or less pronounced decrease in LD/A at 257 nm is observed. This may be due to effects of this type on the optical factor but may also have its origin in a decreased orientation due to compaction and aggregation (since in the case of fuchsin, aggregation was observed).

Finally a comparison between the spectroscopic and "free ligand" determinations of the stabilities: a Scatchard plot based on a partition study of MG + DNA at low ionic strength (fig. 8) yielded $K_1 = 1.8 \times 10^6$ M^{-1}, $n_1 = 0.15$ and $K_2 = 1 \times 10^5$ M^{-1} ($n_2 = 0.10$). This result should be compared with that obtained by computational minimization of the differences between the observed LD and those calculated by means of eqs. (8), (9), (12) and (13) by free variation of the unknown parameters (the result is displayed in fig. 9). The considerably higher K_2 and the very high standard deviations of the evaluation based on the optical observations can be ascribed to an unjustified assump-

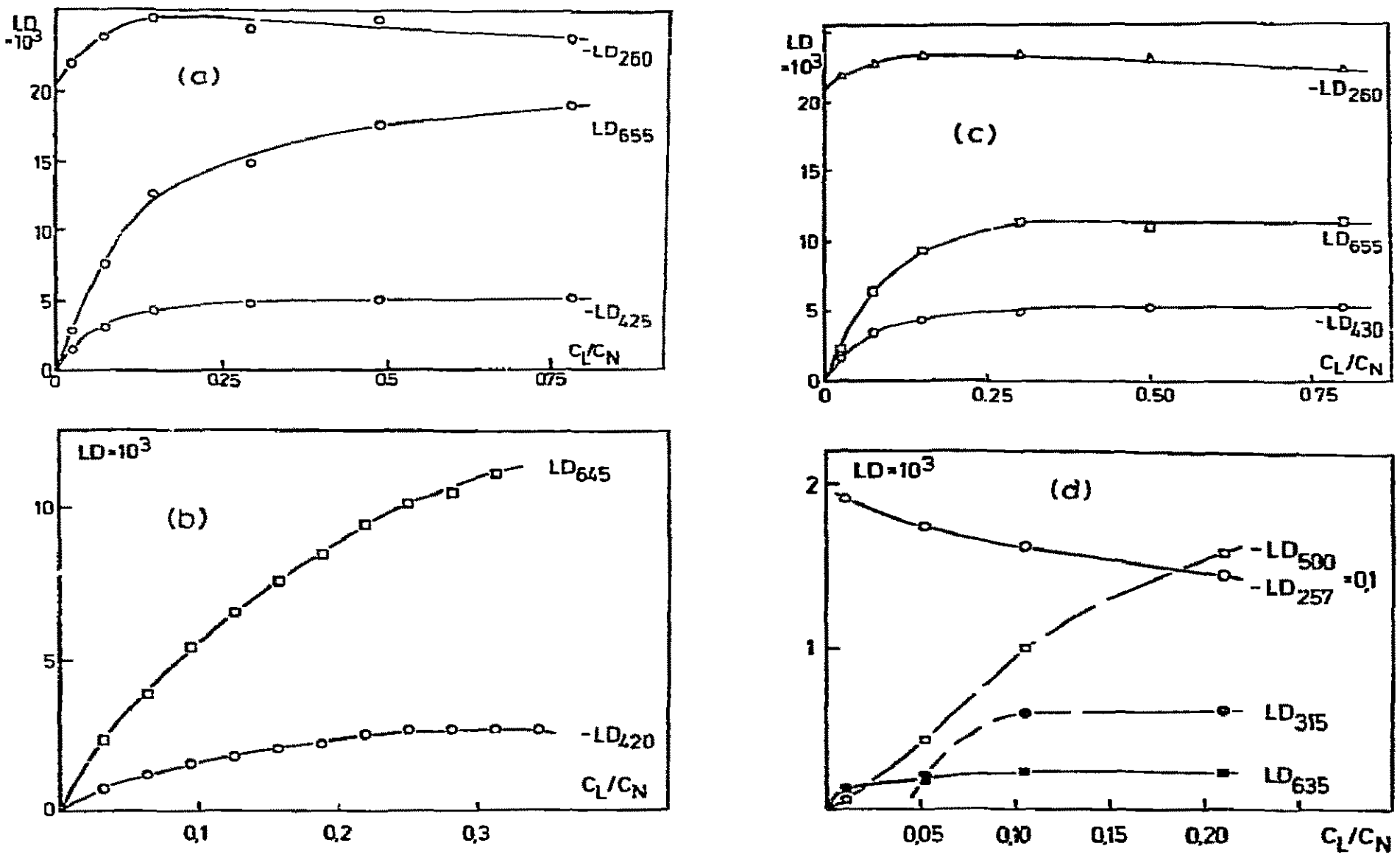

Fig. 7. Titration curves showing LD ($G = 4000\ s^{-1}$, $d = 0.10$ cm) at the extrema as a function of C_L/C_N for: (a) 3-pyridine green ($C_N = 2 \times 10^{-4}$ M, $I = 5 \times 10^{-3}$ M Na^+), (b) o-bromomalachite green ($C_N = 2.9 \times 10^{-4}$ M, $I = 0.1$ M NaCl) and (c) p-nitromalachite green ($C_N = 2.0 \times 10^{-4}$ M, $I = 0.005$ M Na^+), (d) p-fuchsin ($C_N = 1.0 \times 10^{-4}$ M, $I = 0.1$ M Na^+).

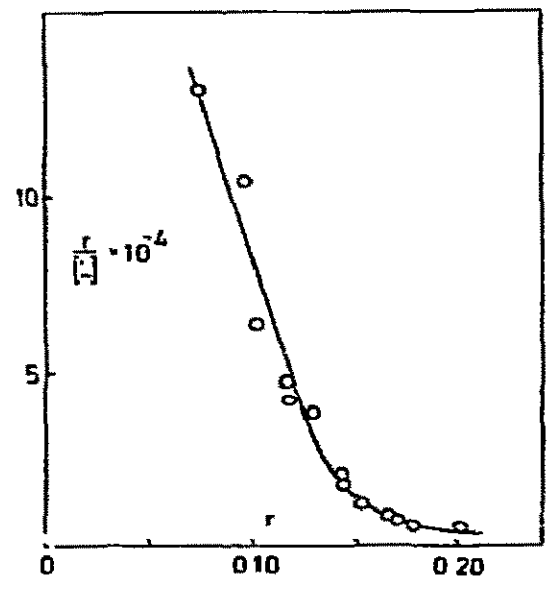

Fig. 8. Example of Scatchard plot based on a partition analysis (MG, $C_N = 1.0 \times 10^{-4}$ M, $I = 0.005$ M Na^+).

tion of constant $\Delta\epsilon_i$ due to exciton coupling. As expected, good agreement between the methods is obtained at the higher ionic strength where no exciton effects were observed.

The structural possibilities for the dye-polynucleotide complexes studied were investigated with the aid of spacefilling models [25] (fig. 10). For this discussion we can summarize our experimental characterisation as follows:

1. The angular orientation of MG with respect to the local helix axis is 20–47° to the x axis and approximately 90° to the z axis. (Eq. (5) gives $F^{do} = 0.103$ from $(LD/A_r)_{257} = -0.154$ and $\langle\theta_x^H\rangle = 47°$ from $(\Delta\epsilon/\epsilon)_{645} = +0.062$ and $\langle\theta_z^H\rangle = 90°$ from $(\Delta\epsilon/\epsilon)_{425} = -0.181$ assuming pure x and z polarizations of the respective bands. The limit value of 35°

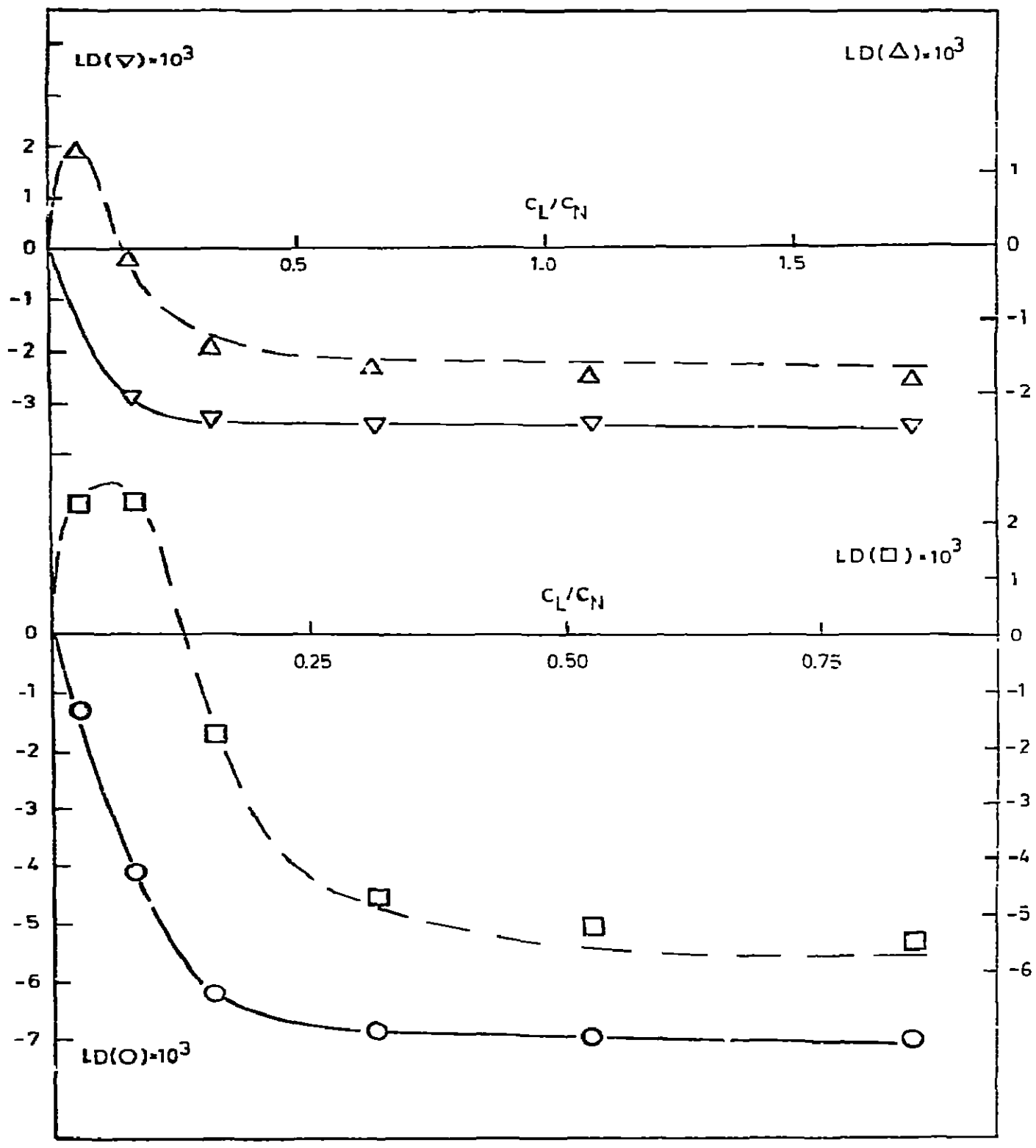

Fig. 9. Example of computational minimization of $|LD_{calc}-LD_{exp}|$ by free variation of K_i, n_i, $\Delta\epsilon_i$ (623 nm), $\Delta\epsilon_i$ (422 nm); $i = 1, 2$. LD_{exp}, the experimental LD at 623 nm (△ $C_N = 9.15 \times 10^{-5}$ M; □ $C_N = 1.93 \times 10^{-4}$ M) and at 422 nm (▽ $C_N = 9.15 \times 10^{-5}$ M; ○ $C_N = 1.93 \times 10^{-4}$ M), is compared with the calculated (broken lines for 623 nm, full lines for 422 nm). Resulting parameters: $K_1 \times 10^{-6}/M^{-1} = 1.43 \pm 0.78$; $K_2 \times 10^{-6}/M^{-1} = 0.53 \pm 0.40$; $n_1 = 0.06 \pm 0.07$; $n_2 = 0.10 \pm 0.10$; $\Delta\epsilon_1 \times 10^{-3}/M^{-1}\,cm^{-1} = 14.4 \pm 23.1$ (623 nm), -6.5 ± 7.9 (433 nm); $\Delta\epsilon_2 \times 10^{-3}/M^{-1}\,cm^{-1} = -11.7 \pm 10.2$ (623 nm). $\Delta\epsilon_2$ (422 nm) was set to zero.

is obtained by taking into account a possible admixture of up to 30% z in the 645 nm band [23]). The estimated θ values for the other dye complexes are given in table 3.

2. The $(\Delta\epsilon/\epsilon)_{425}$ value is significantly larger than $(\Delta\epsilon/\epsilon)_{257}$ indicating that the dye z axis is on average more nearly perpendicular to the local helix axis than are the base pair planes. This could be due to an increased structural stability (persistency) of regions on the helix which are preferentially covered by dye: the regions not stiffened by dye should explain the lower $(\Delta\epsilon/\epsilon)_{257}$. Another plausible explanation is that the base pairs are not perfectly perpendicular to the helix axis. The observed divergence corresponds to a devia-

Table 3
Angular orientations of the x and z axes of the dye ligands with respect to the local helix axis. F is taken as $-(LD/1.5A)_{257}$, and the limits for θ_x and θ_z polarization of the 640 nm and 430 nm bands

Dye	MG^{2+}	MAG^+	2-TG^+	3-PG^+	p-OH-MAG^+ p-NO_2MAG^+
pseudo symmetry					$C_{2v}(C_2)$
F^{do}	0.102	0.077	0.069	0.115	0.104 0.102
θ_x^H(deg)	35–47	0–49	0–50	0–50	0–49 0–49
θ_z^H(deg)	90	78–90	72–90	71–90	72–90 71–90

Dye	o-CH_3O-MAG^+-CH_3O-MAG^+	o-Br-MAG^+	p-I-MAG^+	$MICH^+$	CV^+ p–F^+
pseudo symmetry					$C_{3v}(D_3)$
F^{do}	0.089	0.086	0.097	0.27[a]	0.1 0.253[a]
θ_x^H(deg)	0–53	0–49	0–51	62–90	> 55 55–60
θ_z^H(deg)	58–90	70–90	72–90	55–90	

[a] In 10% dextran.

tion of at least 13° from perpendicularity. Differences from the ideal Watson-Crick model are not surprising since the molecules studied are in solution.

3. According to the models a possible arrangement in the MG complex is an intercalation of the two equivalent dimethylaminophenyl groups (fig. 10b) This alternative is, however, excluded by the fact that $\langle\theta_x^H\rangle \leqslant 47°$. The bulkiness of the trimethylaminophenyl group is, judged from the models, a severe hindrance to the intercalation of this group. As well, the greater charge density on this amino nitrogen should reduce the relative tendency of this group to be attracted to the hydrophobic base pockets. The fact that a number of dyes with quite different groups along the z axis (2-TG, the para-substituted MAG derivatives) show similar LD also supports the concept that the z dimension is not intercalated. The observation of a decreased $(LD/A)_{425}$ for dyes with crowding substituents, R_2, (particularly o-CH_3O) is also indirect evidence against an intercalated z axis, since these substituents should affect the rotation around the z axis but, most probably, not the orientation of this axis.

4. The protection from enolization suggests that the strongly bound MG (though possibly not the weakly bound) is effectively protected against nucleophilic attack by the negative charges on DNA. A similar protection against diazotization has been reported for aminoacridines when bound to DNA [26].

5. The binding energy is large ($-\Delta G°$ ca 30 kJ mol^{-1}) for most of the dyes. There are several indications that the electrostatic contribution is considerable (the effect of ionic strength, the increase to $-\Delta G° = 40$ kJ mol^{-1} for the divalent dye MG, the general requirement for the ligand to be a cation). However the importance of van der Waals forces also, can be suspected from the apparent requirement of a large net aromatic surface (ca 40 $Å^2$ per dye molecule). These properties are similar to those of the aminoacridine dyes, but these however according to the presently available evidence are intercalated. Fig. 10d shows a non-intercalated structure for MG which would give optimum contact between the dye molecule and the hydrophobic surfaces of the DNA strands. For MG it is probable that the more positively charged trimethylamino group points out towards the phosphates, while for the thiophene and malchite green dyes the equivalently charged dimethylamino groups can be expected to be directed in this way. In both cases the x direction will be oriented at an angle of 40–50° to


H
(a)

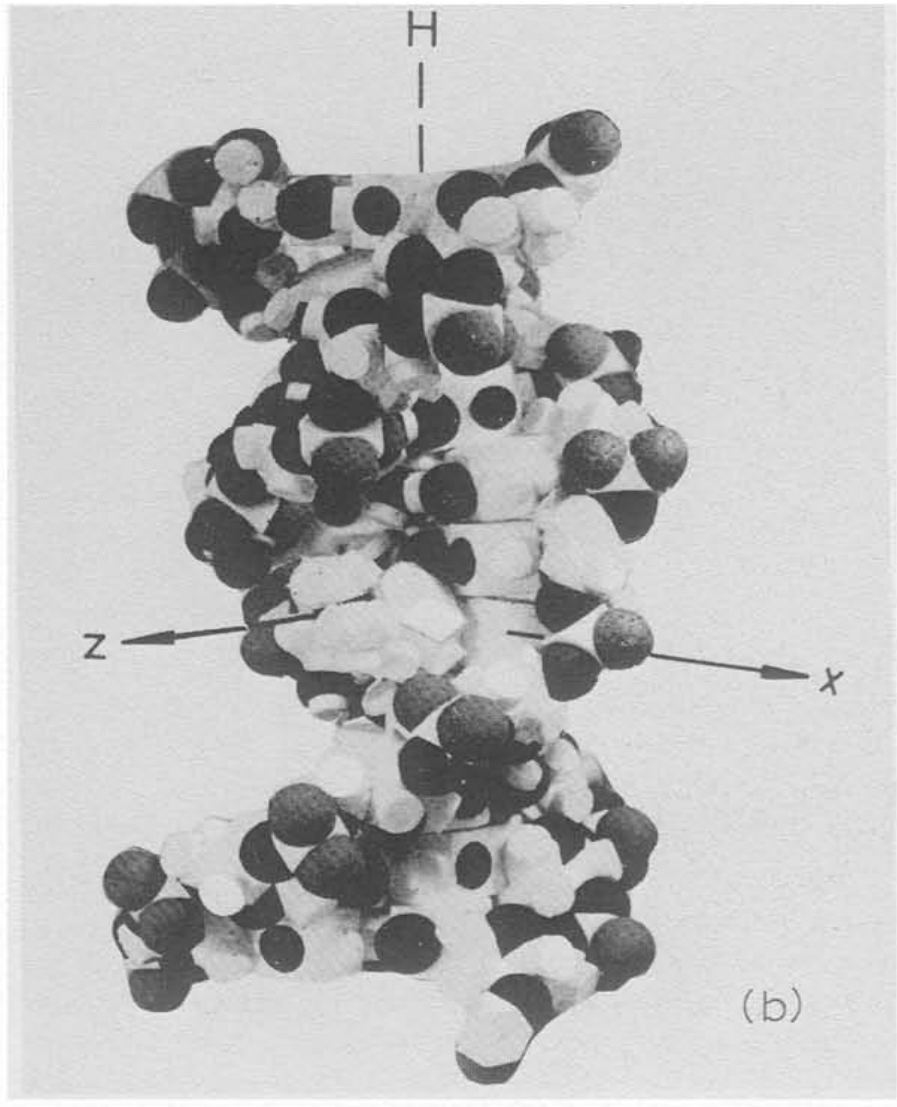
H
z
x
(b)

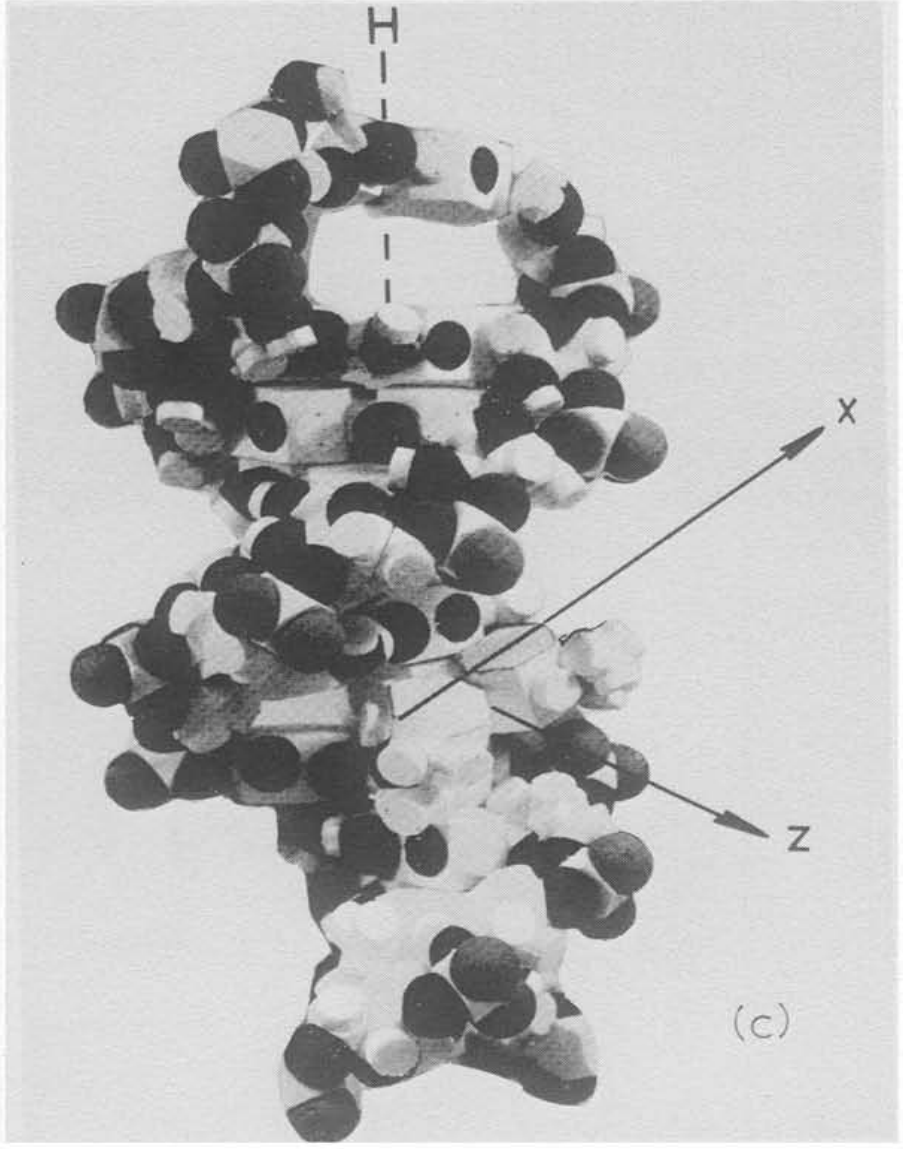
H
x
z
(c)

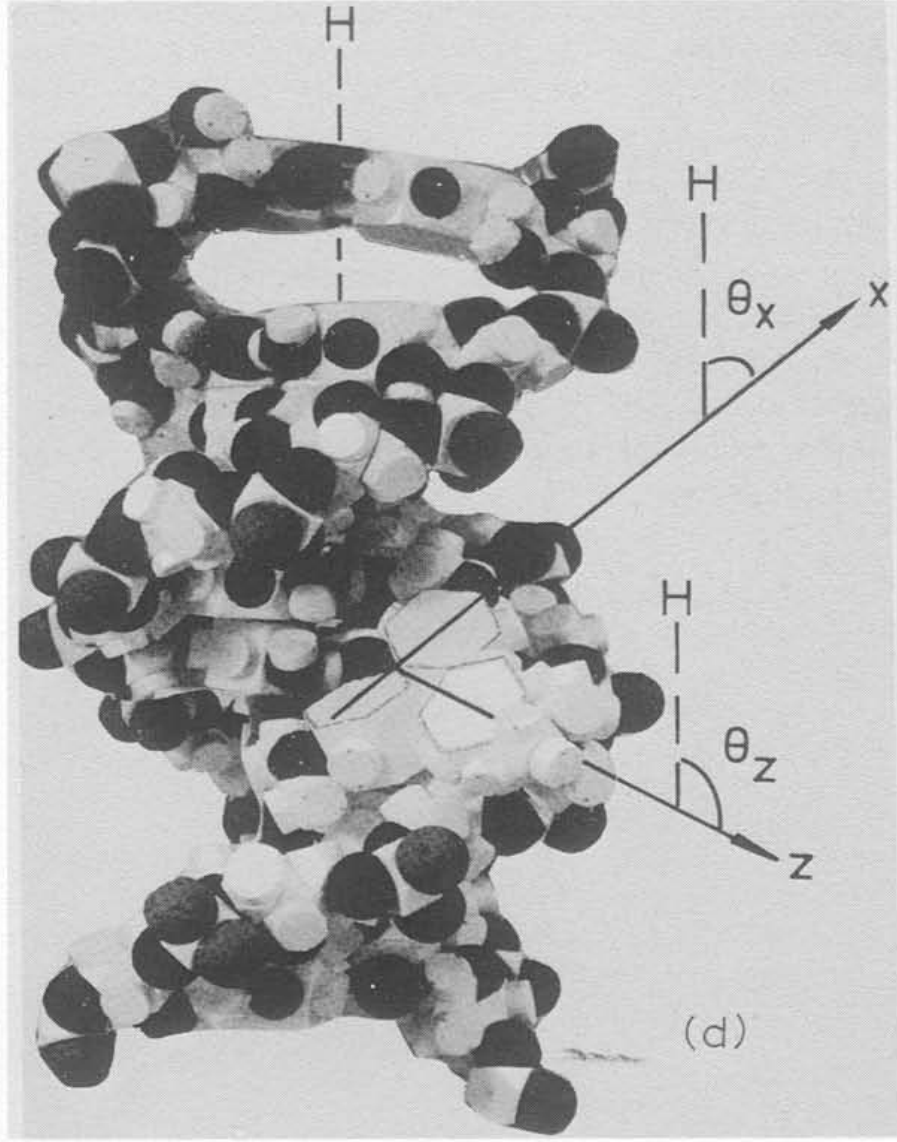
H
H
θx
x
H
θz
z
(d)

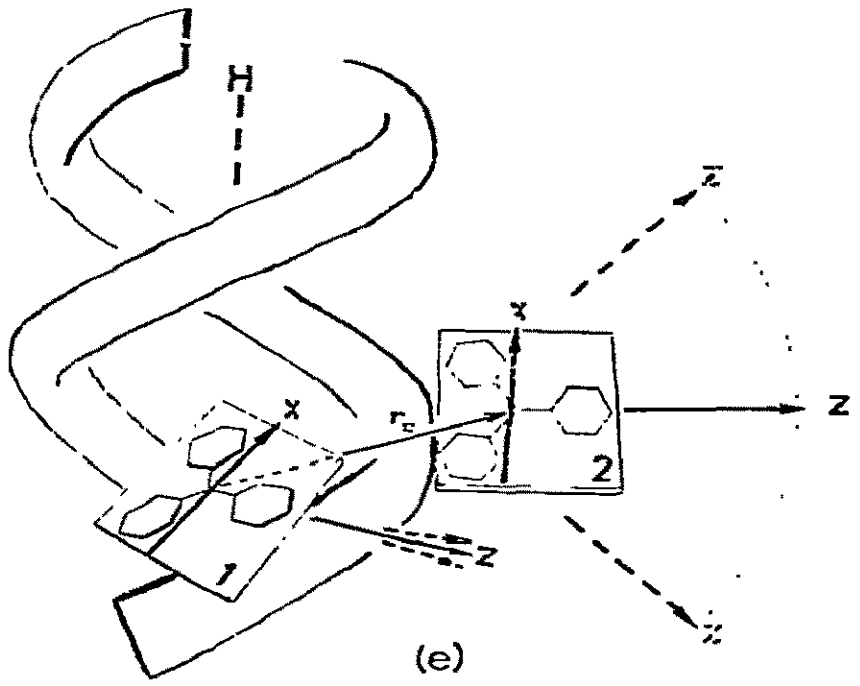

Fig. 10. Possible DNA-dye structures. (a) Probable structure of intercalated ethidium dye: the phenanthridinium ring system is placed in a slot between adjacent base-pairs; the phenyl ring pointing out (arrow) is strongly twisted out of the molecular plane. (b-c) Intercalation alternatives for triphenylmethane dyes: (b) The entire molecule, except for one aromatic ring is contained in a base-pair slot. In the figure it is the trimethylaminophenyl ring of MG that is pointing out along the z axis. (c) Only one ring (that along the z axis) is inserted into a slot. (d) A non-intercalated site in the major groove. This structure is suggested for the C_{2v} (MG) as well as for the C_{3v} (CV) dyes. (e) Peripheral site suggested for a second complex with methyl green.

the helix (H) and the z axis perpendicular to the helix axis, in excellent agreement with the conclusions from the LD observations.

6. The pair of bands of opposite polarizations observed around 650 nm in LD as well as in CD can be understood in terms of exciton coupling between the transition moments in neighbouring MG molecules. This conclusion is strengthened by the very rapid way in which the intensities increase with C_L/C_N (a r_{12}^{-3} dependency can be expected for the interaction energy over the inter-dye distance).

In table 4 the rotational strengths and energy splitting have been calculated for an infinite (right handed) helix of MG molecules arranged according to the structure suggested in fig. 10d (the notations of the geometrical parameters introduced in ref. [13] have been used). The inter-dye distance r_{12} = 14 Å and the values on γ, ρ and ψ correspond to a fairly close packing along one of the grooves. The fact that $LD/A_r F^{do}$ is considerably less than +3.0 for the parallel band indicates a strong mutual overlap between the exciton components and/or a finite number of monomers in the dye helix. In view of this, the experimental rotational strength $R_{\parallel}$ (from the area under the 665 nm CD band) can be considered in good agreement with that estimated for the suggested structure. The theoretical energy separation (2Δ in eq. (10) of ref. [13]) is also in very good agreement with that observed if it is taken into account that the apparent peaks are shifted away from each other by the overlap.

7. A zero exciton CD at 425 nm follows from $\gamma = \theta_x = 0$. However, the structure with a single site does not explain why LD is saturated at 425 nm or why only the divalent MG, and not the other dyes with similar n_1, shows strong exciton CD. A much more satisfactory model can therefore be obtained with a second peripheral site. Even if it is of mainly electrostatic nature it can favour a certain orientation of the dye molecule relative to the polynucleotide strand. With the arangement illustrated in fig. 10e the MG x axis will be essentially oriented as in the first site with respect to the helix direction, H, while the z axis can be considered almost randomly oriented in this respect.

Table 4
Dye-dye interaction in the MG-DNA complex. "Inner" (r = 7Å) and "peripheral" (r = 14Å) site.

Theory [a]								Experiment [b]	
r_{12}/Å	$\gamma=\theta_x$/deg	ρ/deg	σ/deg	ψ/deg	r/Å	Δ/cm^{-1}	$R_{\parallel}/10^{-52}$ rad J m^3	Δ/cm^{-1}	$R_{\parallel}/10^{-52}$ rad J m^3
14	48	50	0	80	7	−389	+9.8	−466	+1.75
14	48	40	0	45	14	−412	+19.4		

a) $R_{\parallel} = R_{\perp} = \pi\nu|\mu|^2 r\,(\sin 2\gamma \cos\sigma)/2$; Δ according to eq. (10) of ref. [13]. $|\mu|^2 = 6.59 \times 10^{-58}$ (Cm)^2 was estimated from the absorption spectrum.
b) $R_{\parallel} = (2.3 \times 10^{-52}/\lambda_{max}) \int (\epsilon_l - \epsilon_r)\,d\lambda$ rad J m^3.

As shown in table 4 this structure can be expected to give rotational strengths and energy splittings of the same magnitudes as those observed.

8. The C_{3v} symmetry dyes (crystal violet and fuchsin) although they are characterized only by negative LD bands do not necessarily have different orientations. To a first approximation the absorption intensity is degenerately polarized in the xz plane and the molecules may be considered as disc-like. The angle, α, that the disc makes to the helix axis is then obtained from the observed LD by means of a modified eq. (5): $\cos^2\theta_i^H$ is replaced by $\frac{1}{2}\cos^2\alpha$ [19]. From the calculated $(\Delta\epsilon/\epsilon)_{555} = -0.19$ for fuchsin we obtained $\alpha = 55°$, in fairly good agreement with the angle the planes of the C_{2v} symmetric dyes make with the DNA axis. Although no corresponding quantitative analysis was possible for crystal violet the general resemblance of the LD spectrum to that of fuchsin strongly suggests a similar orientation.

9. With Michler's hydrol blue a weak negative LD was observed over the entire spectrum. Only a small amount of dye was found to bind to DNA (less than 10% when $C_L = 1.6 \times 10^{-5}$M, $C_N = 2.9 \times 10^{-4}$ M at $I = 0.1$ M Na^+) and the evaluation of $\Delta\epsilon/\epsilon$ was uncertain. θ_x was estimated to be larger than 62° (the band around 600 nm was employed; it has previously been shown to be purely x polarized [23]). A band at 400 nm (with z-polarization [23]) also showed negative LD; taken together the observations indicate that the plane of the molecule is essentially perpendicular to the helix axis. Michler's hydrol blue can thus very well be intercalated.

Concluding remark. As this investigation shows, it is possible to extract fairly detailed structural data from LD via the two-dimensional properties of chromophores such as those studied here. This possibility seems not to have been fully appreciated before and previous studies of complexes with DNA have usually employed LD only as a very qualitative tool.

Acknowledgements

This work was supported by the Swedish Natural Science Research Council (contract no K 3216–006, K3216–009). Dr. Brian Thomas, Organic Chemistry 2, Chemical Center, Lund, is gratefully acknowledged for the loan of his space-filling model system [25].
Dr. Roland Karlsson kindly carried out the computer fitting of the equilibrium parameters to the LD data.

References

[1] A.D. Wolfe, Biochemistry 16 (1977) 30.
[2] A.K. Krey and F.E. Hahn, Biochemistry 14 (1975) 5061.
[3] W. Müller and F. Gautier, Eur. J. Biochem. 54 (1975) 385.
[4] L.D. Zeleznik and C.M. Sweeney, Arch. Biochem Biophys. (1976) 292.
[5] E. Fredericq and C. Houssier, Electric dichroism and electric birefringence (Clarendon Press, Oxford 1973) p. 129.
[6] A. Wada, in: Applied spectroscopy reviews, Vol. 6, ed. E.G. Brame (M. Dekker, New York, 1973) p. 1.
[7] G.R. Kelly and T. Kurucsev, Biopolymers 15 (1976) 1481.
[8] C. Houssier, B. Hardy and E. Fredericq, Biopolymers 13 (1974) 1141.
[9] A.I. Poletayev, FEBS Lett. 67 (1976) 171.
[10] F.E. Hahn and A.K. Krey, Antimicrob. Agents Chemother. 1968 (1969) 15.
[11] K. Yamaoka and H. Hashimoto, Chem. Lett. 1976 (1976) 465.
[12] B. Nordén and F. Tjerneld, Biophys. Chem. 4 (1976) 191.
[13] B. Nordén and F. Tjerneld, Biophys. Chem. 6 (1976) 31.
[14] B. Nordén and F. Tjerneld, Chem. Phys. Letters 50 (1977) 508.
[15] A. Peterlin and H.A. Stuart, Z. Physik 112 (1939) 129.
[16] H.J. Hofrichter and J.A. Schellman, in: The Jerusalem Symposia on Quantum Chemistry (The Israel Academy of Sciences and Humanities, Jerusalem, 1973).
[17] H. Scheraga, J. Edsall and J. Gadd, J. Chem. Phys. 19 (1951) 1101.
[18] R. Wilson and J.A. Schellman, to be published.
[19] B. Nordén, in: Problems of contemporary biophysics (The Polish Scientific Publishing Company, Warszawa, 1977).
[20] P.-Å. Albertsson, Partition of cell particles and macromolecules, 2nd edition (Wiley, 1971).
[21] V.P. Shanbhag, R. Sodergård, H. Carstensen and P.-Å. Albertsson, J. Steroid Biochem. 4 (1973) 537.
[22] G. Bengtsson, Acta Chem. Scand. 23 (1969) 435.
[23] Å. Davidsson and B. Nordén, Chem. Scr. 11 (1978) 68.
[24] D.G. Dalgleish, H. Fujita and A.R. Peacocke, Biopolymers 8 (1969) 633.
[25] B.R. Thomas, Biochimie 55 (1973) 1325.
[26] L.S. Lerman, J. Mol. Biol. 10 (1964) 367.